

EPTT-2022-0041

Analysis of the boundary layer intermittence and turbulent transition due to a gap.

Felipe Oliveira Aguirre¹
Marlon Sproesser Mathias²
Marcello A. F. Medeiros¹

felipe.aguirre@usp.br
marlon.mathias@usp.br
marcello@sc.usp.br

¹São Carlos School of Engineering - University of São Paulo

²Institute of Advanced Studies - USP

Abstract. *The interaction of the boundary layer with small surface irregularities has been studied in several contexts. Several studies reveal that some configurations of small cavities, also called gaps, can induce boundary-layer disturbances due to the presence of unstable hydrodynamic modes. The literature presents results where, in some scenarios, the presence of gaps can induce boundary layer transition, more specifically, via the bypass transition phenomenon. To better understand this scenario, a representative case was chosen, where turbulence begins after a transition zone along the length of the flat plate. For this case, it was analyzed how the unstable modes predicted in linear stability theory behave in the flow. Initially, it was investigated how these modes behave inside the cavity, interacting and subsequently being convected out of the cavity. Subsequently, the convected structures were followed along the domain, to understand if there is memory of the flow structures present inside the cavity. We observed the presence of unsteady two-dimensional modes in the mixing layer, known as Rossiter modes, and unstable three-dimensional modes inside the cavity, known as centrifugal modes, which are subsequently convected into the boundary layer downstream of the cavity. Analyzing the intermittent region, where the flow oscillates between turbulent and laminar, it was possible to notice that the Rossiter and Centrifugal modes are present in this region, interacting with each other. Finally, through the analysis of the turbulent region, it is possible to note the presence of memory of the centrifugal modes present in the cavity, as well as the presence of residual modes with a frequency close to the Rossiter modes.*

Keywords: *boundary layer, flow instability, transition to turbulence, DNS, open cavity*

1. INTRODUCTION

In this work we study a boundary layer flow over an open cavity whose dimensions are, usually, one order of magnitude larger than the boundary layer thickness.

According to more recent work, the situation closest to the reality of an aircraft in flight would be the introduction of a disturbance in the boundary layer upstream of the cavity or roughness, this is a way of imitating naturally occurring Tollmien-Schlichting waves. Therefore, the irregularities should not act as generators of the disturbance, but instead modify the waves already present in the flow Crouch and Ng (2000); Plogmann *et al.* (2014); de Paula *et al.* (2017). Taking into account this context of cavities more in line with reality, Crouch *et al.* (2020) identified a parametric region in their experiments where an abrupt change of behavior of the flow occurs, where a phenomenon of anticipation of the transition point occurs abruptly, this is called by *bypass transition*.

Recent studies by the group have observed that in cases where *bypass transition* occurred, both two-dimensional unsteady modes (Rossiter modes) and three-dimensional unsteady modes (Centrifugal modes) were found Mathias (2021).

The Rossiter modes, in short, are self-sustained disturbances in the mixing layer and are amplified up to the trailing edge, where when they collide with the trailing edge, they generate an acoustic wave, which returns through the interior of the cavity exciting the mixing layer once more Rossiter (1964). The centrifugal modes, on the other hand, are the modes connected to the recirculation inside the cavity, with defined spanwise periods, therefore being three-dimensional Bres and Colonius (2008). It was also possible to observe similar behavior for the linear instability analysis, for Mach 0.5, well above the Mach at which the experiment was performed (below 0.1).

2. METHODOLOGY

For the present study, an unstable case was chosen. This case was chosen based on previous studies, where a parameter sweep was performed resulting in the choice of an intermediate case to two cases studied earlier in the group (Mathias and Medeiros, 2019). The case in question was non-dimensionalized by the displacement thickness of the boundary layer at the cavity's leading edge (δ_0^*), and by the free-flow velocity. Also follows the following definitions: length-depth ratio (L/D) equal to 2, as well as a depth of $6.11 \delta^*$. The cavity is situated at a Re^* of 734, with Mach equal to 0.9.

The case was simulated using a Direct Numerical Solver for the Navier-Stokes equations (DNS). The DNS was developed by the group and written in Fortran 90, and it solves Navier Stokes' compressible equations. For the spatial resolution, a sixth order Compact Finite Difference Schemes with Spectral-like method was used, and for the buffer zones, the explicit fourth-order method was used. For the temporal resolution, the fourth-order Runge-Kutta method was used. Fig. 1 contains a section of the X Y plane, to exemplify the operation of the mesh.

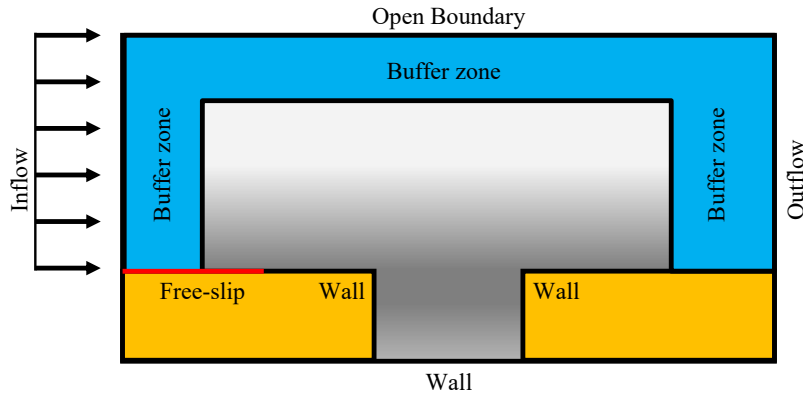


Figure 1. Illustrative image of the computational domain, the buffer zones are in blue.

The stability analysis code was also developed by the group (Mathias and Medeiros, 2018). It uses linear stability theory (LST) (Theofilis, 2011) to confirm whether the case in question would be stable or unstable, as well as the unstable modes that should be observed in the 3D DNS.

With the stability analysis, it was possible to observe the unstable modes, as well as to set up the domain so that it was possible to have a resolution of 4 points per period of the mode with the shortest unstable wavelength, as well as a domain with 4 periods of the mode with the longest unstable wavelength.

With the results obtained in DNS, two-dimensional sections of the flow were also used to analyze this flow. To better understand the transition, it is necessary to analyze not only whether the case has transitioned or not, it is necessary to look carefully at the modes present in each part of the domain, for this, spectrum analyses were performed to understand whether the modes predicted in the LST are present in the cavity, as well as whether the modes present in the cavity also appear downstream, as well as to what extent they are present and how they change as we move towards the end of the domain.

The computational domain in the flow direction is about 25 cavity lengths in size, this is needed so that there is enough space for the intermittent region to form. This region alone occupies about 12 cavity lengths, as the transition moves over time.

3. RESULTS

The case chosen for this study is in the boundary between marginal instability and a fully unstable flow (Mathias and Medeiros, 2019). Initially, it was necessary to determine which modes were unstable, and with that determine the domain span-wise length that would be sufficient to capture all unstable modes present in the flow. LST determined the major unstable modes for each span-wise wave number (β) chosen.

The modes found are shown in Fig. 2. Initially, looking at the amplification, we have that for β/π between 0.1 and 1 there are several unstable modes, of the centrifugal type, as well as the presence of a two-dimensional mode (Rossiter mode) for $\beta/\pi = 0$. We have the frequencies of the dominant modes as predicted for the three-dimensional modes (Bres and Colonius, 2008).

To facilitate the comparison between the physical domain and the spectral domain, we will change the span-wise wave number from β to $1/\lambda$, given by $1/\lambda = \beta/2\pi$, where $1/\lambda$ is equivalent to the inverse of the wavelength in the span-wise direction. The spanwise wavenumber expected for the centrifugal 1 is around $0.25 \leq 1/\lambda \leq 0.5$. For the centrifugal 2 is expected a spanwise wavenumber around $0.15 \leq 1/\lambda \leq 0.2$. Finally the centrifugal 3 is expected for $0.7 \leq 1/\lambda \leq 0.1$.

The analysis of the mixing layer, for $Y \approx 0.1$, we have in Fig. 3, again the energy concentration in low-frequency modes is in frequency modes 0, and in frequencies in the range of Rossiter predicted in the LST. Again, the higher frequency modes concentrate a lot of energy, making it necessary to perform filtering to observe the low-frequency modes.

We can see the presence of velocity fluctuations, near the trailing edge region, for the same spanwise position along with the time in the physical domain filtered Fig. 4, without the high frequencies. We can also observe that a deformation of the vortices occurs in physical space, suggesting an interaction between stationary and non-stationary centrifugal modes within the, gap. Analyzing the modes present in the mixing layer, filtering the high-frequency modes, it can be seen in Fig. 4, that the C1 mode has a value of $1/\lambda$ different from that observed in the LST. It is also possible to observe the

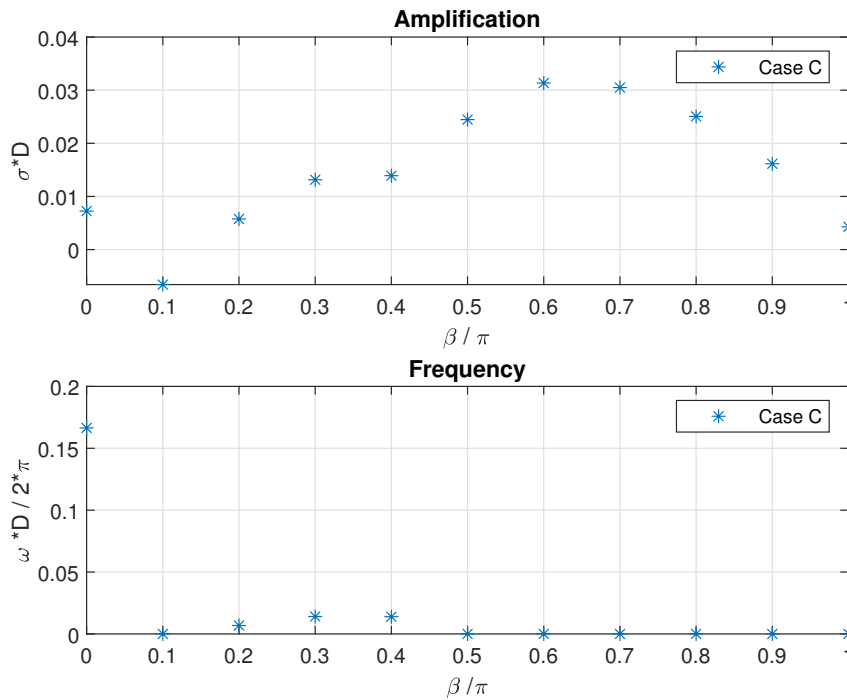


Figure 2. LST prediction for amplification rate of unstable modes.

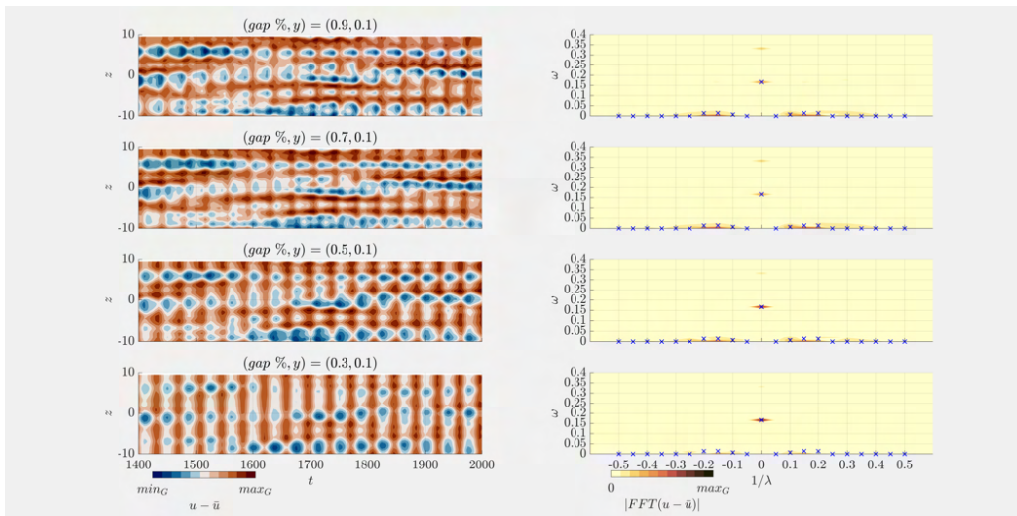


Figure 3. In the left column we have the physical domain and in the right column the respective 2D spectral domain for for different percentages of the gap in X, at a height of $Y \approx 0.1$. The blue markings are the most unstable modes predicted by the LST for each value of $1/\lambda$.

presence of energy in the range of modes C2 and C3.

Analyzing the bottom of the cavity, for $Y \approx -5.5$, in the Fig. 5, we see that for the initial three-quarters of the gap, the energy concentrates in the low-frequency range, as well as in the range predicted by the LST for Rossiter mode 1. However, the energy concentrated in the Rossiter 1 make it difficult to visualize the centrifugal modes, as can be seen in Fig. 5.

Filtering the high-frequency modes, in Fig. 6, in the initial three-quarters of the gap, the energy concentration in stationary C1 modes is visible. Now, in the physical domain, we can see the presence of vortices that move in the spanwise direction over time near the trailing edge. Close to the leading edge, we have modes that move in the spanwise direction with a much lower speed, showing only a deformation in the flow vortices. In the center of the gap, we can notice an intermediate behavior, where the two behaviors are present together. The C1 mode is in the range close to that predicted by the LST. It is also possible to visualize the presence of low-frequency modes, with frequencies similar to LST, in the range of $1/\lambda$ near to the C2 and C3 modes.

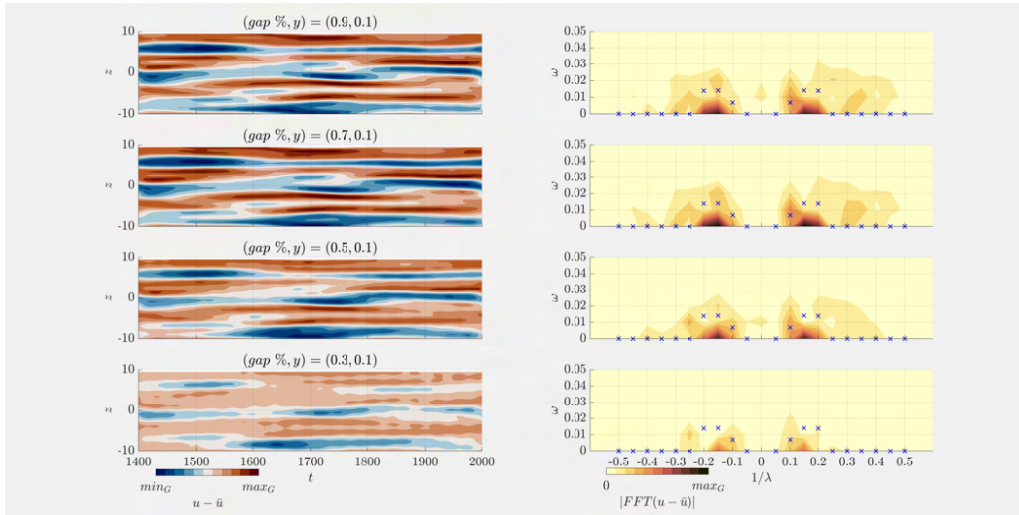


Figure 4. In the left column we have the physical domain and in the right column the respective 2D spectral domain for for different percentages of the gap in X, at a height of $Y \approx 0.1$, filtering the high-frequencies. The blue markings are the most unstable modes predicted by the LST for each value of $1/\lambda$.

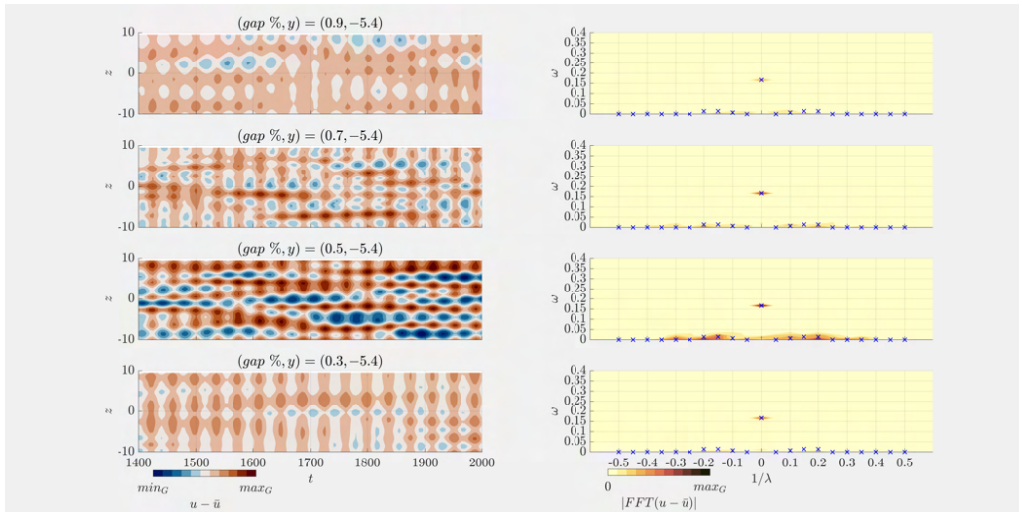


Figure 5. In the left column we have the physical domain and in the right column the respective 2D spectral domain for for different percentages of the gap in X, at a height of $Y \approx -5.4$. The blue markings are the most unstable modes predicted by the LST for each value of $1/\lambda$.

Moving on to an analysis of the vortices present in the gap, we can observe in Fig. 7 the presence of three-dimensional structures very different from those observed in the previous cases, structures more irregular than those observed so far.

For the 2D cut, in Fig. 8, we can notice the presence of very different structures from those found in the laminar boundary layer, structures that are related the turbulence present in the case.

In Fig. 8, the transition region of the boundary layer as indicated in the figure by dotted black lines, was observed over different simulation times. These small oscillations present in this case cavity amplify as we move downstream.

At $t = 1950$, Fig. 9, we observe that there is a movement at the point where the flow becomes turbulent, being upstream of the point observed in 8.

The changes in the transition point presented above occur throughout the simulation, indicating that there is an intermittence in the transition point, which in this case corresponds to a region of about 15 cavity lengths in the X direction upstream of the cavity.

For this case, Rossiter modes interfere substantially with the visualization of three-dimensional modes. It was necessary to perform filtering of high-frequency modes.

Initially, analyzing the spectra, we can notice that in the region close to the trailing edge, the modes appear to be consistent with the predicted by the LST, with the energy concentrated in the range of C1 and R1 modes. As we follow the gap downstream to the beginning of the transition region, we have Rossiter modes dominating the flow. As we continue further downstream, towards the center of the transition region ($X \approx 380$) the low-frequency modes come to dominate the flow. Which can be seen in Fig. 10.

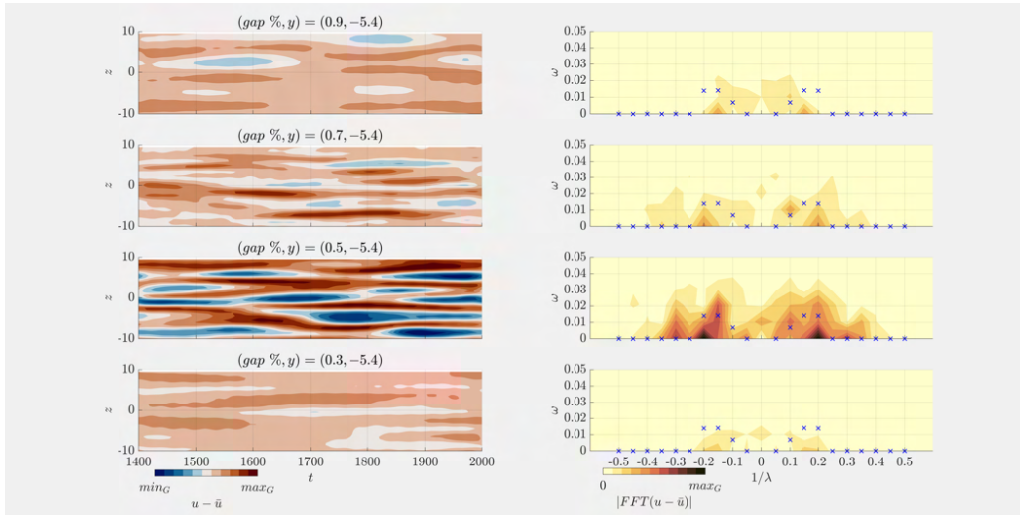


Figure 6. In the left column we have the physical domain and in the right column the respective 2D spectral domain for different percentages of the gap in X , at a height of $Y \approx -5.4$, filtering the high-frequencies. The blue markings are the most unstable modes predicted by the LST for each value of $1/\lambda$.

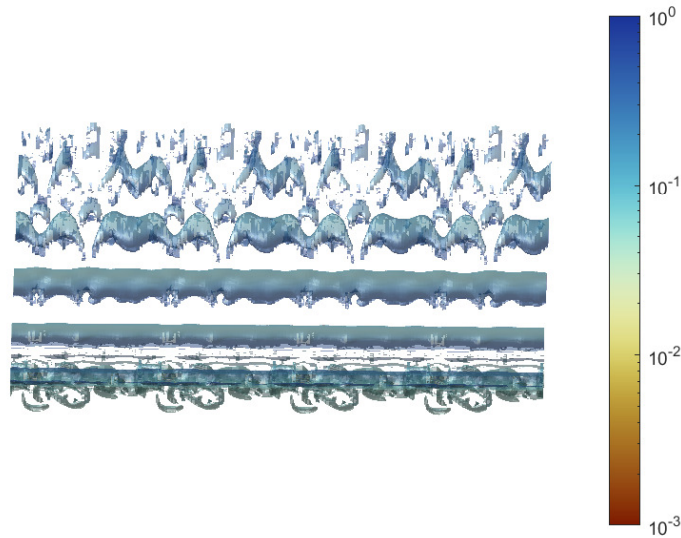


Figure 7. Q-criterion isosurfaces snapshots, where it is possible to observe the vortices present inside the gap and convected. Domain in spanwise direction was replicated 4 times for better visualization. The figure is in the gap region.

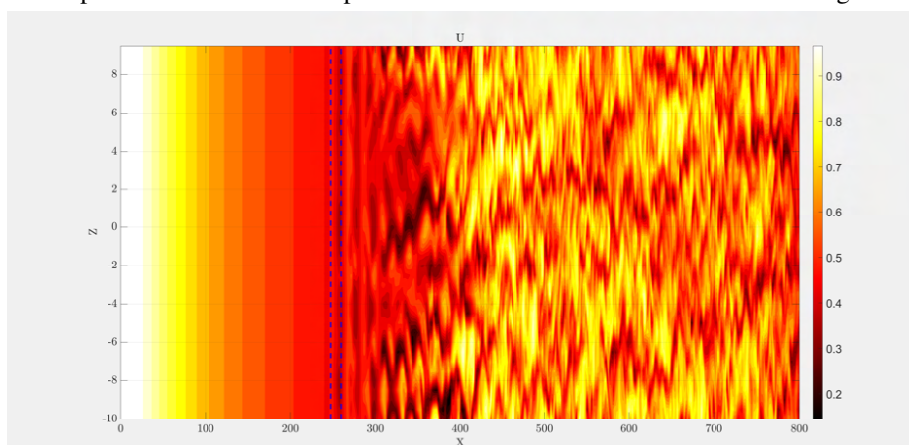


Figure 8. Flow cut in the $Y = 1$ plane to the velocity component U , at time $t = 1800$.

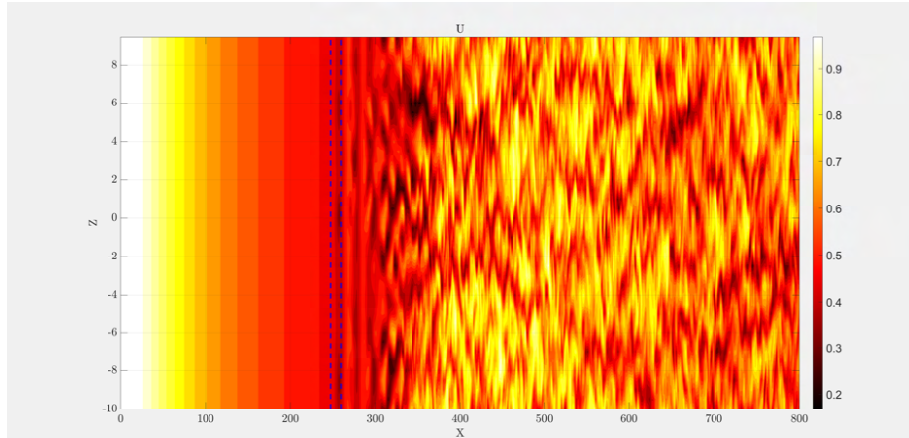


Figure 9. Flow cut from in the $Y = 1$ plane to the velocity component U , at time $t = 1950$.

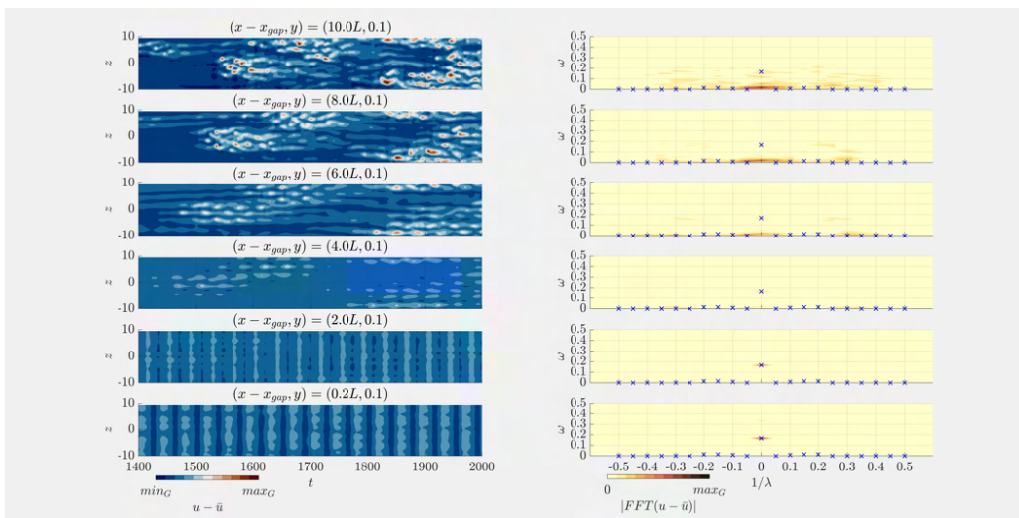


Figure 10. In the left column we have the physical domain and in the right column the respective 2D spectral domain for different positions of X downstream of the gap before the fully developed turbulence, at a height of $Y \approx 0.1$. For this case $L/\delta^* = 12.22$. The blue markings are the most unstable modes predicted by the LST for each value of $1/\lambda$.

In Fig. 11, where the high-frequency modes are filtered out, we can see the presence of fluctuations near the gap in well-defined positions in the spanwise direction, which as we advance downstream, we can see that the fluctuations begin to oscillate over time in the spanwise direction. We can better observe how the centrifugal modes, in the region close to the trailing edge, and in the center of the boundary layer transition region. We can observe close to the trailing edge of the gap, we can notice the presence of modes similar to those expected by the LST (C1 and C2). As we move downstream, modes with higher $1/\lambda$ become more relevant, as well as changes in the baseflow, modes with $1/\lambda = 0$ and a frequency different from 0. The observed change in the baseflow dominates the intermediate portion of the transition region.

In Fig. 12, where the high-frequency modes are filtered out, in the region where the flow is already three-dimensional, we can see that the physical space velocity fluctuations become more and more random, keeping few characteristics of the gap. At the end of the transition region and in the turbulent transition region and the turbulent region, the modifications in the base flow continue to dominate and the flow has no memory of Rossiter modes, as well as little energy in modes other than those present in this flow.

As observed, in the viscous sublayer, we no longer have a great concentration of energy in the modes predicted by the LST.

As we advance downstream, there is a spreading of energy along the frequency of the Rossiter modes, for values of $1/\lambda$ equivalent to the centrifugal modes observed in the gap, however, this energy starts to concentrate again in a mode with low frequency and $1/\lambda = 0$, again indicating a change in base flow.

By filtering the high-frequency modes, in Fig. 14, we can notice that close to the gap, still have fluctuations in well-defined positions in the spanwise region. Downstream of the gap, we have that the flow starts to change to regions that oscillate more and more in the spanwise direction over time. As well can better observe the behavior of the low-frequency modes in the same region. In Fig. 14, we can see that the centrifugal modes near the trailing edge start to change as we walk downstream. The change is gradual, where the modes spread to various frequencies and various wavenumbers.

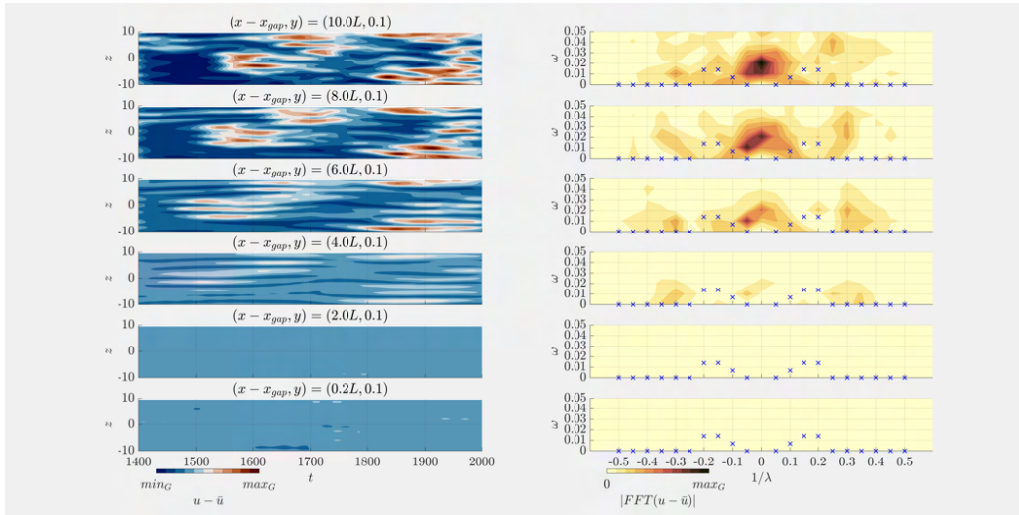


Figure 11. In the left column we have the physical domain and in the right column the respective 2D spectral domain for different positions of X downstream of the gap before the fully developed turbulence, at a height of $Y \approx 0.1$, without the highest frequencies. For this case $L/\delta^* = 12.22$. The blue markings are the most unstable modes predicted by the LST for each value of $1/\lambda$.

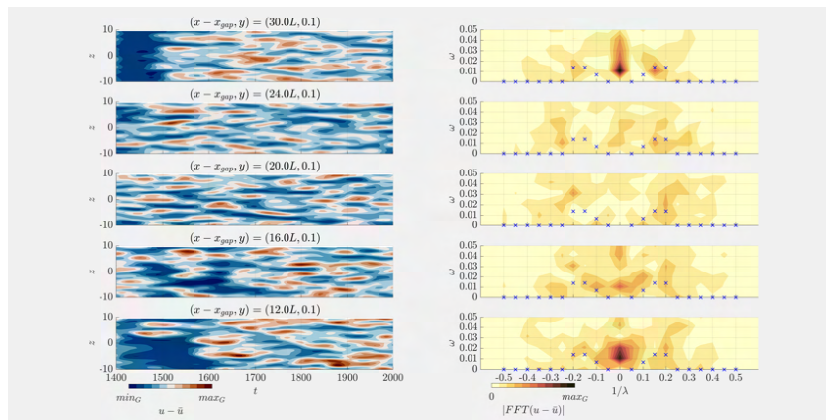


Figure 12. In the left column we have the physical domain and in the right column the respective 2D spectral domain for different positions of X downstream of the gap in the turbulent region, at a height of $Y \approx 0.1$, without the highest frequencies. For this case $L/\delta^* = 12.22$. The blue markings are the most unstable modes predicted by the LST for each value of $1/\lambda$.

Subsequently, after this cascade, the energy is concentrated around a mode with $1/\lambda = 0$ at the center of the transition region.

Despite the concentration of energy in one mode, there is still a lot of energy spread to various wavenumbers along the region of spanwise wavenumbers of centrifugal modes.

Towards the end of the transition region and turbulent region, Fig. 15, we have that the velocity fluctuations become more and more similar to a turbulent flow, losing a good part of the characteristics observed inside the gap. The energy of the modes is concentrated in a mode with $1/\lambda = 0$, loosely reminding of the two-dimensional cavity modes, however, there is still a small amount of energy close to that of the centrifugal modes predicted in the LST.

4. CONCLUSION

We studied the transition to turbulence in a flat plate with a globally unstable cavity. For this case, the instability modes found in the cavity with a DNS, were compared to those predicted in the theory of linear stability (LST), we were specially interested on how these modes behave during the transition process of the boundary layer.

The wall law, as well as the friction coefficient, were used to confirm the transition process, as well as the help of two-dimensional cuts and figures using the Q-criterion and λ_2 were used to visualize the structures and try to understand the behavior. With the figures of the flow and vortices, it was possible to notice that there is a transition region, where the flow is not fully turbulent, but also not laminar. The presence of a relatively long region of intermittency for the transition point may be related to the degree of instability of the case.

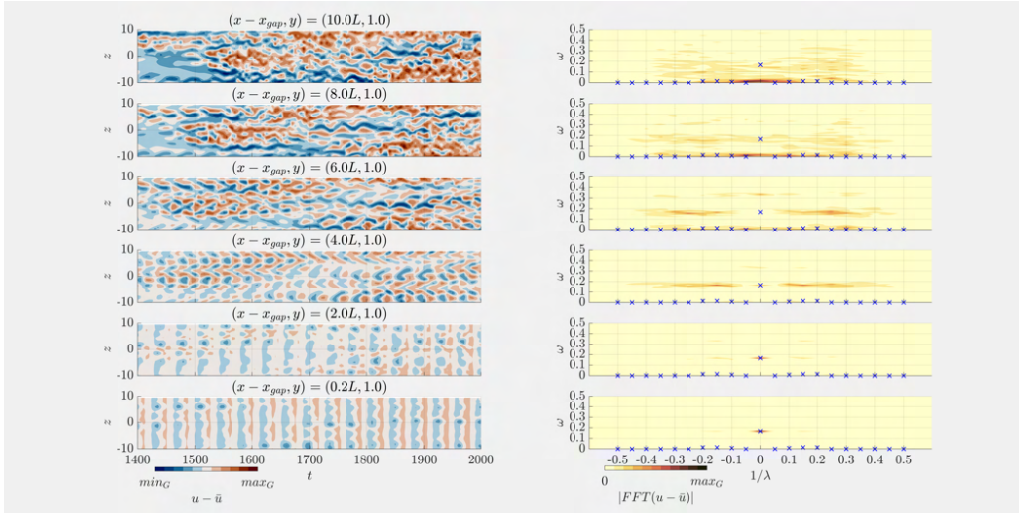


Figure 13. In the left column we have the physical domain and in the right column the respective 2D spectral domain for different positions of X downstream of the gap before the fully developed turbulence, at a height of $Y \approx 1$. For this case $L/\delta^* = 12.22$. The blue markings are the most unstable modes predicted by the LST for each value of $1/\lambda$.

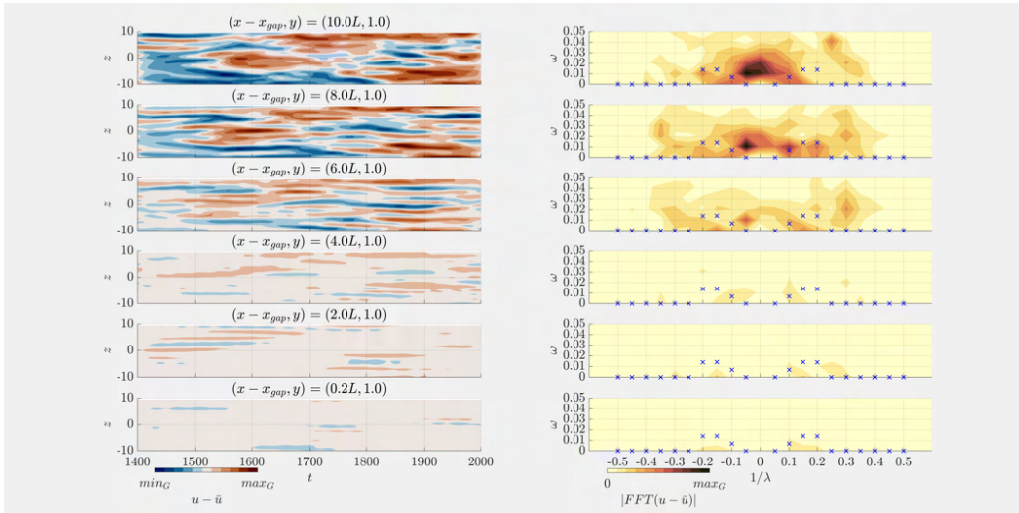


Figure 14. In the left column we have the physical domain and in the right column the respective 2D spectral domain for different positions of X downstream of the gap before the fully developed turbulence, at a height of $Y \approx 1$, without the highest frequencies. For this case $L/\delta^* = 12.22$. The blue markings are the most unstable modes predicted by the LST for each value of $1/\lambda$.

The LST predicted the existence of centrifugal modes of type II and III for the region of $0 < \beta/\pi < 0.5$ as the most unstable for these betas, while for $0.5 < \beta/\pi < 1$ the presence of stationary centrifugal modes were predicted as the most unstable for these betas. For $\beta/\pi = 0$ a Rossiter mode was expected. However, in DNS, stationary modes were not observed, with the flow dominated only by non-stationary modes. The centrifugal modes of $0 < \beta/\pi < 0.5$ have a frequency similar to that predicted in the LST, and the observed Rossiter mode is also similar to that expected by the LST.

The 2D spectra also revealed that the 2D modes underwent a three-dimensionalization in the same β/π region as the existing centrifugal modes. It was also observed that during the transition region it is possible to observe the presence of the modes found in the gap. Another important point observed is that in the turbulent region, despite the frequency scattering, the spectrum remains in the β/π region of the cavity modes.

Finally, using the observed spectra and using the Q-criterion figures to help the interpretation, we can see that the interaction of two-dimensional modes with the three-dimensional ones present in the cavity is responsible for generating the three-dimensionality observed in the turbulent region of the boundary layer. Nothing can be said about which mode is responsible for the transition, but it is reasonable to say that the interaction of unstable centrifugal modes with also unstable Rossiter modes can generate three-dimensionality in the boundary layer, which can therefore lead to the boundary layer transition.

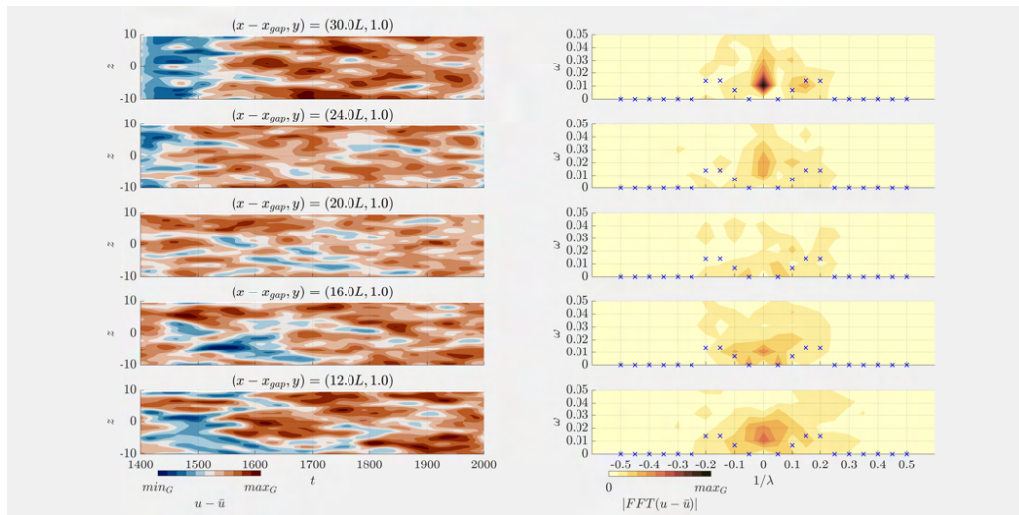


Figure 15. In the left column we have the physical domain and in the right column the respective 2D spectral domain for different positions of X downstream of the gap in the turbulent region, at a height of $Y \approx 1$, without the highest frequencies. For this case $L/\delta^* = 12.22$. The blue markings are the most unstable modes predicted by the LST for each value of $1/\lambda$.

5. ACKNOWLEDGEMENTS

M.S.M is sponsored by FAPESP (grant no. 2018/04584-0). M.A.F.M. is sponsored by CNPq/Brazil (grant no. 307956/2019-9), sponsored by FAPESP (grant no. 2019/15336-7) and the US Air Force Office of Scientific Research (AFOSR) for grant FA9550-18-1-0112, managed by Dr. Geoff Andersen from SOARD; the University of Liverpool for the access to the Barkla cluster, provided by Prof. Vassilios Theofilis; and the Center for Mathematical Sciences Applied to Industry (CeMEAI) funded by São Paulo Research Foundation (FAPESP/Brazil), grant 2013/07375-0, for access to the Euler cluster, led by Prof. José Alberto Cuminato.

6. REFERENCES

- Bres, G.A. and Colonius, T., 2008. “Three-dimensional instabilities in compressible flow over open cavities”. *JOURNAL OF FLUID MECHANICS*, Vol. 599, pp. 309–339. ISSN 0022-1120. doi:10.1017/S0022112007009925.
- Crouch, J.D. and Ng, L.L., 2000. “Variable n-factor method for transition prediction in three-dimensional boundary layers”. *AIAA Journal*, Vol. 38, No. 2, pp. 211–216. doi:10.2514/2.973. URL <https://doi.org/10.2514/2.973>.
- Crouch, J.D., Kosorygin, V.S. and Sutanto, M.I., 2020. *Modeling Gap Effects on Transition Dominated by Tollmien-Schlichting Instability*, AIAA AVIATION FORUM. doi:10.2514/6.2020-3075. URL <https://arc.aiaa.org/doi/abs/10.2514/6.2020-3075>.
- de Paula, I.B., Würz, W., Mendonça, M.T. and Medeiros, M.A.F., 2017. “Interaction of instability waves and a three-dimensional roughness element in a boundary layer”. *Journal of Fluid Mechanics*, Vol. 824, p. 624–660. doi: 10.1017/jfm.2017.362.
- Mathias, M.S., 2021. *Computational study of the hydrodynamic stability of gaps and cavities in a subsonic compressible boundary layer*. Ph.D. thesis, University of São Paulo.
- Mathias, M.S. and Medeiros, M., 2018. “Direct numerical simulation of a compressible flow and matrix-free analysis of its instabilities over an open cavity”. *Journal of Aerospace Technology and Management*, Vol. 10, p. 13. ISSN 1984-9648. doi:10.5028/jatm.v10.949.
- Mathias, M. and Medeiros, M.F., 2019. *Global instability analysis of a boundary layer flow over a small cavity*, AIAA Aviation 2019 Forum. doi:10.2514/6.2019-3535. URL <https://arc.aiaa.org/doi/abs/10.2514/6.2019-3535>.
- Plogmann, B., Würz, W. and Krämer, E., 2014. “On the disturbance evolution downstream of a cylindrical roughness element”. *Journal of Fluid Mechanics*, Vol. 758, p. 238–286. doi:10.1017/jfm.2014.499.
- Rossiter, J.E., 1964. “Wind-tunnel experiments on the flow over rectangular cavities at subsonic and transonic speeds”. *Reports and Memoranda No. 3438 - Aeronautical Research Council - Ministry of Aviation*.
- Theofilis, V., 2011. “Global linear instability”. *Annual Review of Fluid Mechanics*, Vol. 43, No. 1, pp. 319–352. doi: 10.1146/annurev-fluid-122109-160705. URL <https://doi.org/10.1146/annurev-fluid-122109-160705>.

7. RESPONSIBILITY NOTICE

The following text, properly adapted to the number of authors, must be included in the last section of the paper:

Aguirre, F. O., Mathias, M. S. and Medeiros, M. A. F.
Analysis of the boundary layer intermittence and turbulent transition due to a gap.

The author(s) is (are) the only responsible for the printed material included in this paper.